Asia-Pacific Journal of Science and Technology :Volume :31 Issue :03 Article ID :APST-31-03-01 Research Article

APST

Asia-Pacific Journal of Science and Technology

https//:www.tci-thaijo.org/index.php/APST/index

Published by Research and Innovation Department,
Khon Kaen University, Thailand

Influence of Host Matrix on Optical Properties of Samarium-Doped Glasses: A Comparative Analysis of Zinc Oxide and Zinc Fluoride

Wiraphat Thanyaphirak[1, 2], Patarawagee Yasaka[1, 2, *], Kitipun Boonin[1, 2] and Jakrapong Kaewkhao[1, 2]

[1] Physics Program, Faculty of Science and Technology, Nakhon Pathom Rajabhat University, Nakhon Pathom, 73000, Thailand
[2] Center of Excellence in Glass Technology and Materials Science (CEGM), Nakhon Pathom Rajabhat University, Nakhon Pathom 73000, Thailand
[*]Corresponding author: pyasaka@webmail.npru.ac.th

Received 4 June 2025
Revised 20 January 2026
Accepted 4 February 2026

Abstract

Samarium-doped glasses have attracted considerable interest due to their promising optical properties for use in photonic, laser, and optoelectronic applications. In this work, a comparative study was conducted on Sm^{3+}-doped borotellurite glasses with the chemical composition $29TeO_2–30B_2O_3–10X–20BaO–10Nb_2O_5–1Sm_2O_3$, where X represents either ZnO or ZnF_2. The influence of the modifier type (oxide vs. fluoride) on the structural and luminescence behavior of the glasses was thoroughly examined. The incorporation of Sm^{3+} ions into these host matrices leads to significant variations in optical performance, dictated by the local environment and bonding characteristics. Comprehensive characterization, including absorption and emission spectra, and luminescence lifetimes, was performed to evaluate the suitability of each glass system for optical device applications. The findings highlight the critical role of glass composition in tailoring the emission efficiency and optical response of rare-earth-doped glass materials.

Keywords: Borotellurite, ZnO, ZnF_2, Samarium

1. Introduction

Rare-earth-doped glasses have attracted substantial attention in the fields of photonics, solid-state lasers, optical amplifiers, and display technologies due to their ability to exhibit sharp emission lines, long fluorescence lifetimes, and efficient radiative transitions. Among the rare-earth ions, samarium (Sm^{3+}) is of particular interest because of its ability to emit intense orange-red luminescence, which is highly desirable for applications in visible light-emitting devices, laser media, and optical sensors.

The choice of glass matrix plays a critical role in modulating the local environment around the dopant ions, thus influencing their spectroscopic behavior. Tellurite-based glasses (TeO_2) are known for their high refractive indices, excellent rare-earth ion solubility, extended infrared transmission, and relatively low phonon energy (~750 cm^{-1}) [1], which reduces non-radiative losses and enhances luminescence efficiency. Boron oxide (B_2O_3) acts as a strong glass former that improves the specific physical and chemical durability of the host network [2], while also facilitating good rare-earth dispersion due to its low viscosity and high rare-earth solubility.

Barium oxide (BaO) serves as a network modifier that breaks the random network of glasses [3]. Niobium pentoxide (Nb_2O_5) introduces high field strength and acts as an intermediate oxide, improving the nonlinear optical properties, stabilizing the amorphous network, and increasing thermal stability [4]. Furthermore, Nb_2O_5 can promote the formation of highly polarizable Nb–O bonds that affect local asymmetry, thus enhancing electric dipole transitions.

Zinc oxide (ZnO) is a widely used modifier that contributes to the low rates of crystallization and increases the glass-forming ability [5]. It also enhances glass transparency and offers moderate field strength around dopant ions. In contrast, zinc fluoride (ZnF_2) introduces significant structural and optical changes due to its high

electronegativity, low phonon energy, and ionic bonding characteristics [6]. The incorporation of fluoride lowers the phonon energy of the host, which can suppress multiphonon relaxation processes and enhance radiative transitions of rare-earth ions. Samarium oxide (Sm_2O_3) is introduced as the active luminescence center. Its intra-4f transitions, particularly from the $^4G_{5/2}$ excited state, give rise to distinct emission bands in the visible region. However, these transitions are strongly influenced by the symmetry and rigidity of the surrounding glass matrix.

In this study, borotellurite glasses with the composition $29TeO_2–30B_2O_3–10X–20BaO–10Nb_2O_5–1Sm_2O_3$ (where X = ZnO or ZnF_2) were synthesized to comparatively evaluate the influence of oxide and fluoride modifiers on the physical and optical behavior of Sm^{3+} ions. Although fluoride incorporation is generally expected to reduce phonon energy and enhance radiative efficiency according to theoretical considerations, the actual optical response of Sm^{3+} ions in amorphous glass matrices can deviate from idealized models due to complex structural rearrangements, local field variations, and modifier–network interactions. Through a detailed investigation of structural, absorption, emission, chromaticity, and lifetime properties, this work aims to understand how the modifier type governs the local environment and spectroscopic performance of Sm^{3+} in borotellurite glass matrices, with potential implications for visible photonic applications.

2. Materials and methods

Sm^{3+}-doped borotellurite glasses with the nominal molar composition of $29TeO_2–30B_2O_3–10X–20BaO–10Nb_2O_5–1Sm_2O_3$ (where X = ZnO or ZnF_2) were synthesized using the conventional melt-quenching technique. High-purity analytical grade chemicals—TeO_2 (Sigma Aldrich 99.95%), H_3BO_3 (KEMAUS 99.8%), $BaCO_3$ (HIMEDIA 99.00%), Nb_2O_5 (KEMAUS 99.8%), ZnO (KEMAUS 99.00%) (or ZnF_2 (KEMAUS 99.00%)), and Sm_2O_3 (KEMAUS 99.95%)—were used as starting materials. Boric acid (H_3BO_3) was employed as a source of B_2O_3 due to its ease of decomposition upon heating. Precisely weighed raw materials were mixed in a crucible with 10 grams and melted in an electric furnace at 1150 °C for 1.30 hours under ambient atmosphere. The melt was then rapidly quenched by pouring onto a pre-heated graphite mold. The obtained glass was immediately annealed at 350°C for 3 hours to relieve internal stress, followed by slow cooling to room temperature.

The density (ρ) of the prepared glasses was measured at room temperature using the Archimedes principle with distilled water as the immersion medium. Molar volume (V_m) was calculated using the molecular weight and experimental density values. The refractive index (n) of the samples was determined using a Presidium Refractive Index Meter II. To confirm the amorphous nature of the glasses, X-ray diffraction (XRD) patterns were recorded in the 2θ range of 10°–80° using a Rigaku SmartLab diffractometer with Cu-Kα radiation. The absorption spectra in the range of 400–1800 nm were obtained using a Shimadzu UV-3600 UV-VIS-NIR spectrophotometer. The excitation spectra, emission spectra, and Fluorescence lifetime were measured with an Agilent Cary Eclipse fluorescence spectrometer. CIE chromaticity coordinates were calculated from the emission spectra using standard color-matching functions.

3. Results and discussion

3.1 Density, molar volume, and refractive index

The measured physical properties of the samarium-doped borotellurite glasses—specifically density, molar volume, and refractive index—are presented in Table 1 for both zinc oxide (TBZnO) and zinc fluoride ($TBZnF_2$) host matrices. The density of $TBZnF_2$ glass (4.0226 g/cm³) was notably higher than that of TBZnO (3.7881 g/cm³). This can be attributed to the incorporation of heavier fluoride ions in the $TBZnF_2$ system compared to oxygen in TBZnO, which increases the overall mass per unit volume of the glass. Additionally, the replacement of ZnO with ZnF_2 leads to a denser packing arrangement due to the lower polarizability and smaller ionic radius of F^- compared to O^{2-} [7]. Conversely, the molar volume of $TBZnF_2$ (33.819 cm³/mol) was lower than that of TBZnO (35.912 cm³/mol), indicating a more compact structural arrangement in the fluoride-containing glass [7]. The reduction in molar volume reinforces the notion that ZnF_2 contributes to a tighter glass network, likely due to the stronger ionic character and less deformable bonds of fluorides, which reduce the average free volume in the matrix. The refractive index values for TBZnO and $TBZnF_2$ were relatively close, with TBZnO at 1.6522 and $TBZnF_2$ at 1.6534. Despite the minor difference, the slightly higher refractive index in $TBZnF_2$ could be attributed to the increased density and stronger field strength of fluoride ions, which influence the electronic polarizability and, consequently, the optical dispersion characteristics of the glass. These results collectively indicate that substituting ZnO with ZnF_2 significantly affects the glass structure by increasing density and compactness without drastically altering the refractive index. Such structural modifications may influence the radiative and non-radiative processes associated with Sm^{3+} ions, which will be discussed further in the optical characterization sections.

Table 1 Comparison of Density, molar volume, and refractive index between TBZnO and $TBZnF_2$

Sample	Density	Molar volume	Refractive index
TBZnO	3.7881	35.912	1.6522
$TBZnF_2$	4.0226	33.819	1.6534

3.2 X-ray Diffraction

The amorphous nature of the synthesized samarium-doped borotellurite glasses was confirmed through X-ray diffraction (XRD) analysis, as illustrated in Figure 1. The XRD patterns of both TBZnO and $TBZnF_2$ samples exhibited broad humps without any sharp or distinct crystalline peaks in the 2θ range of 10°–80°, characteristic of an amorphous glassy network [8]. The absence of long-range order in both samples indicates successful glass formation, regardless of the modifier used. However, subtle variations in the shape and width of the amorphous halo between TBZnO and $TBZnF_2$ may suggest differences in the short-range structural arrangement. These differences can be ascribed to the substitution of ZnO with ZnF_2, which alters the bonding environment within the borotellurite network. The presence of ZnF_2, with its lower polarizability and higher ionic character, may lead to a more rigid and compact glass structure, aligning with the previously observed increase in density and decrease in molar volume.

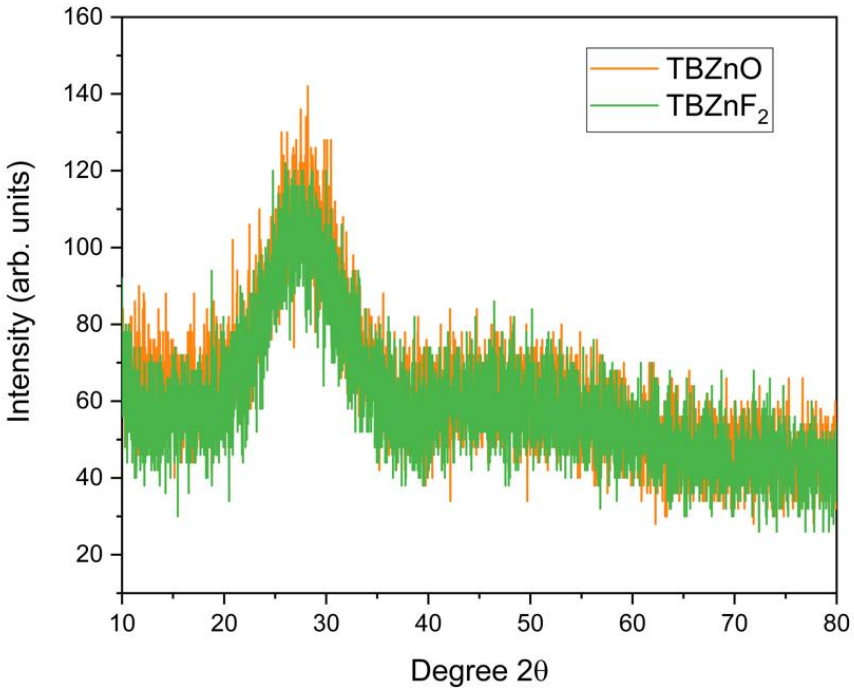


Figure 1 XRD patterns of glass samples comparing zinc oxide and zinc fluoride.

3.3 Absorption

The UV–Vis–NIR absorption spectra of samarium-doped borotellurite glasses modified with ZnO and ZnF_2 are illustrated in **Figure 2**. Both glass systems exhibit several well-defined absorption bands corresponding to the intra-$4f^5$ transitions of Sm^{3+} ions from the ground state $^6H_{5/2}$ to higher excited levels. The near-infrared (NIR) absorption spectra of Sm^{3+}-doped borotellurite glasses with ZnO and ZnF_2 modifiers are shown in **Figure 2**, covering the spectral range from 900 to 1800 nm. The observed absorption bands in this region correspond to intra-4f transitions from the ground state $^6H_{5/2}$ of Sm^{3+} ions to excited states, which are characteristic of rare-earth ion behavior in amorphous hosts. Specifically, the absorption bands observed include: 944 nm: $^6H_{5/2} \rightarrow {}^6F_{11/2}$, 1083 nm: $^6H_{5/2} \rightarrow {}^6F_{9/2}$, 1235 nm: $^6H_{5/2} \rightarrow {}^6F_{7/2}$, 1379 nm: $^6H_{5/2} \rightarrow {}^6F_{5/2}$, 1472 nm: $^6H_{5/2} \rightarrow {}^6F_{3/2}$, 1534 nm: $^6H_{5/2} \rightarrow {}^6H_{15/2}$ [9]. All of these bands are attributed to parity-forbidden 4f transitions, which gain intensity via mixing with opposite parity states due to the local field asymmetry within the glass.

Furthermore, it is important to note that no significant absorption peaks were observed in the visible region (400–800 nm) of either glass sample, making it challenging to directly identify suitable excitation wavelengths for emission measurements based solely on the recorded absorption spectra. This absence may be attributed to the

relatively weak intensity of allowed transitions within this spectral range due to the forbidden nature of 4f–4f transitions and the modest asymmetry present in both glass matrices.

As a result, the selection of excitation wavelengths for photoluminescence measurements was not based on direct absorption data from this study but instead guided by previously reported works on Sm^{3+}-doped glasses with similar host compositions. By referencing literature sources [10] that documented strong excitation peaks—typically observed in the 400–480 nm range, particularly the $^6H_{5/2} \rightarrow {}^4F_{7/2}$ transition around 402–410 nm—appropriate excitation wavelengths were identified and used to excite the samples and obtain their corresponding emission spectra.

This comparative approach ensured that the excitation conditions used in this study were aligned with established standards for Sm^{3+} spectroscopy and optimized to probe the most probable and intense radiative transitions, despite the lack of visible-range features in the absorption measurements. The detailed emission response under these conditions is discussed in the subsequent section.

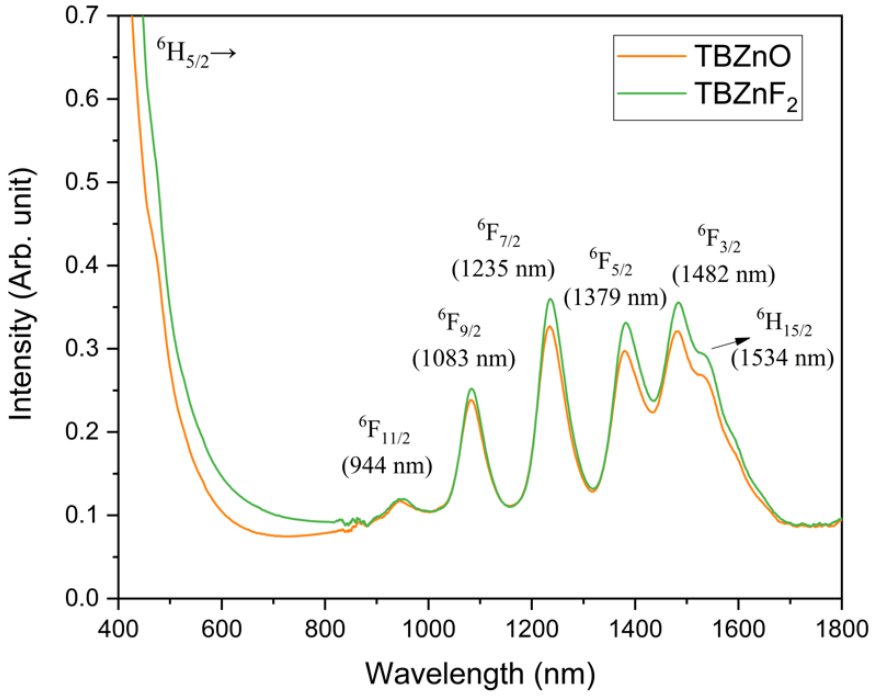


Figure 2 Absorption spectra of glass samples comparing zinc oxide and zinc fluoride.

The optical absorption edge of the Sm^{3+}-doped borotellurite glasses was further analyzed using the Urbach rule, which using the equation provided in the literature [11]. Where the Urbach energy, representing the width of the localized states in the band gap and serving as a measure of structural disorder and electron–phonon interaction in amorphous materials. Figure 3 shows the variation of ln (α)as a function of photon energy for TBZnO and $TBZnF_2$ glasses. The linear regions in the low-energy absorption tails were fitted to extract the Urbach energies. The obtained values are 0.441 eV for TBZnO and 0.435 eV for $TBZnF_2$, respectively. It was found that lower Urbach's energy values lead to less asymmetry, and this asymmetry also affects the emitted light from the glass [12]. This is an important factor that may explain why the emitted light of the glass does not always follow the phonon energy.

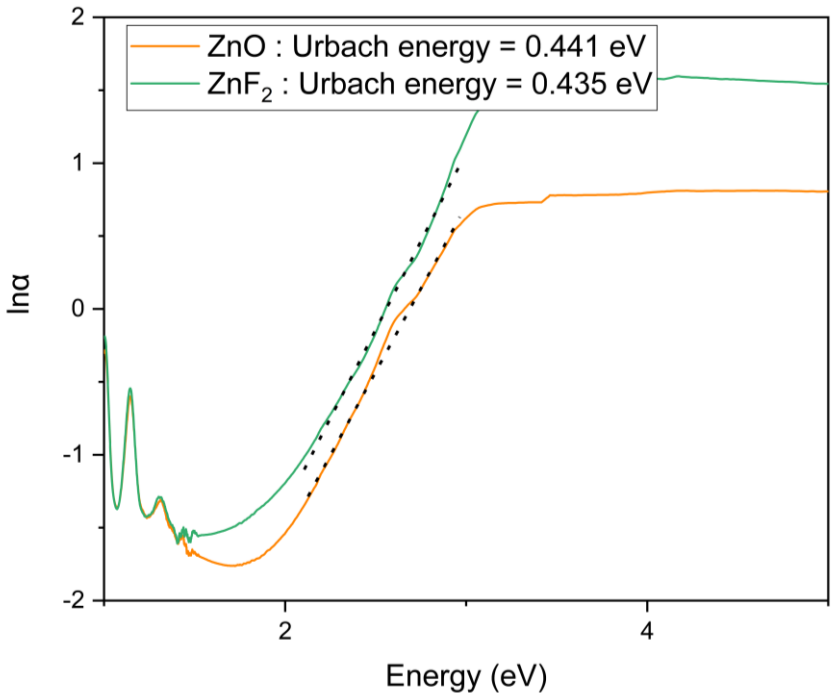


Figure 3 Plot of lnα against photon energy for direct band gap measurement of glass samples comparing zinc oxide and zinc fluoride.

3.4 Excitation and emission spectra

The excitation and emission spectra of the samarium-doped borotellurite glasses modified with ZnO and ZnF_2 are shown in **Figures 4** and **5**, respectively. Due to the absence of a clear absorption band in the visible region (400–800 nm) as observed in the absorption study, the appropriate excitation wavelength cannot be directly determined from the experimental absorption spectra. Therefore, the emission wavelength was selected based on the previously reported study of Sm^{3+} doped glasses [13], using a wavelength of 600 nm. The excitation peaks were observed as $^6H_{5/2} \rightarrow {}^4D_{3/2}$ (362 nm), $^6H_{5/2} \rightarrow {}^6P_{7/2}$ (376 nm), $^6H_{5/2} \rightarrow {}^4F_{7/2}$ (404 nm), $^6H_{5/2} \rightarrow ({}^6F, {}^4P)_{5/2}$ (418 nm), $^6H_{5/2} \rightarrow {}^4I_{15/2}$ (439 nm), $^6H_{5/2} \rightarrow {}^4I_{13/2}$ (464 nm), and $^6H_{5/2} \rightarrow {}^4I_{11/2}$ (476 nm), and the peak at 404 nm was found to be the highest intensity, and was used to investigate the emission peaks..

Upon excitation at 404 nm, both TBZnO and $TBZnF_2$ samples exhibit characteristic emission bands of Sm^{3+} ions, which arise from radiative transitions from the $^4G_{5/2}$ excited state to lower-lying ^6H_J (J = 5/2, 7/2, 9/2, 11/2) levels. The prominent emission transitions observed include: 564 nm: $^4G_{5/2} \rightarrow {}^6H_{5/2}$ (green-orange, weak), 600 nm: $^4G_{5/2} \rightarrow {}^6H_{7/2}$ (orange, hypersensitive transition), 645 nm: $^4G_{5/2} \rightarrow {}^6H_{9/2}$ (red), and 707 nm: $^4G_{5/2} \rightarrow {}^6H_{11/2}$ (deep red) [14]. Among these, the orange emission at 600 nm corresponding to the $^4G_{5/2} \rightarrow {}^6H_{7/2}$ transition was the most intense in both glass samples, which is typical due to its hypersensitive nature and strong electric dipole contribution, especially in asymmetrical environments.

When comparing the two host matrices, TBZnO exhibited marginally higher emission intensity than $TBZnF_2$. This difference may be attributed to the slightly higher asymmetry following the Urbach value and polarizability within the oxide-based glass, which enhances the electric dipole transition probabilities of Sm^{3+} ions. However, the difference in emission strength is not substantial, suggesting that both oxide and fluoride hosts provide relatively comparable local environments for Sm^{3+} ions in terms of luminescence efficiency. These results confirm that both TBZnO and $TBZnF_2$ glasses are capable of supporting visible emissions from Sm^{3+} under near-UV excitation, although their optical response is subtly influenced by the nature of the modifying oxide or fluoride. The findings further validate the effectiveness of literature-guided excitation wavelength selection in the absence of direct absorption guidance in the visible region.

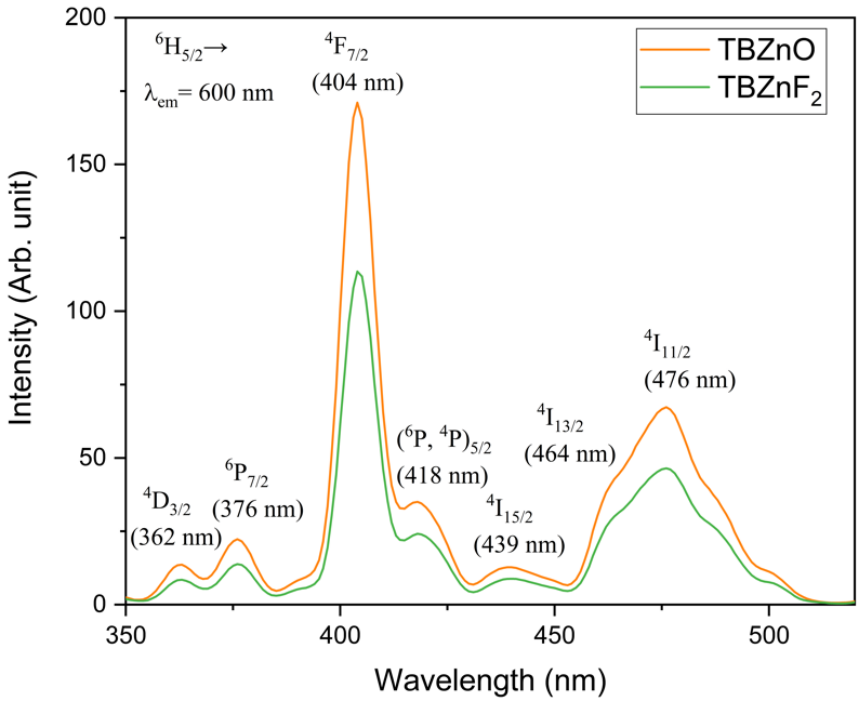


Figure 4 Excitation spectra of glass samples comparing zinc oxide and zinc fluoride.

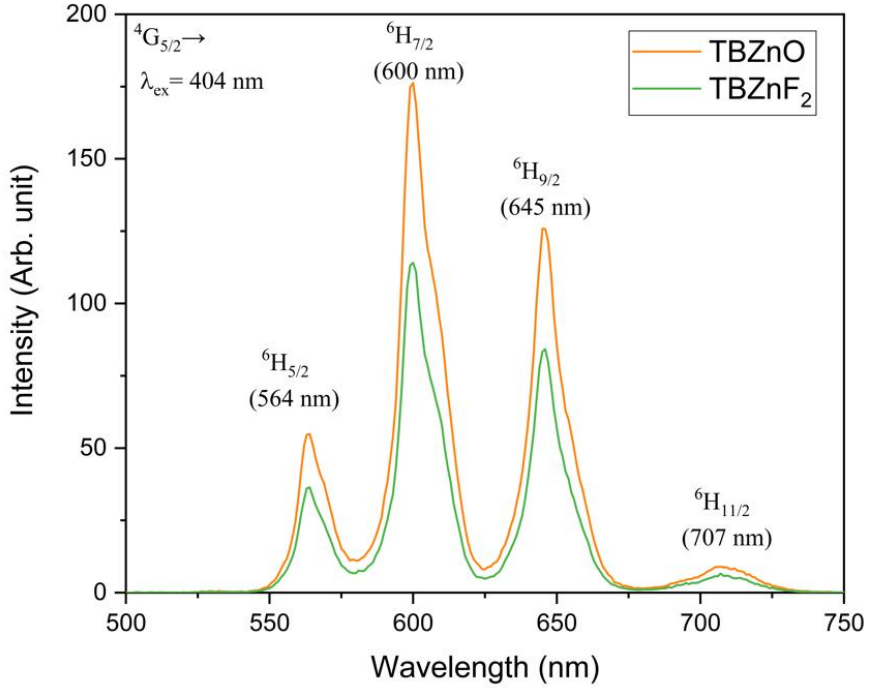


Figure 5 Emission spectra of glass samples comparing zinc oxide and zinc fluoride.

3.5 CIE 1931

The CIE 1931 chromaticity diagram for the Sm^{3+}-doped borotellurite glasses is illustrated in **Figure 6**, which provides a visual representation of the emission color perceived by the human eye. The chromaticity coordinates (x, y) were calculated from the emission spectra using standard color-matching functions and equations reported in the literature [15]. Both TBZnO and $TBZnF_2$ samples exhibit chromaticity coordinates located in the orange-red region of the CIE diagram. This is consistent with the dominant orange emission at 600 nm ($^4G_{5/2} \rightarrow {}^6H_{7/2}$)

and red emission at 645 nm ($^4G_{5/2} \rightarrow {}^6H_{7/2}$), characteristic of Sm^{3+} ions. The color output suggests their suitability for use in warm-colored lighting and photonic applications. The calculated coordinates for TBZnO and $TBZnF_2$ are closely positioned, reflecting the similar emission spectral profiles observed in both samples.

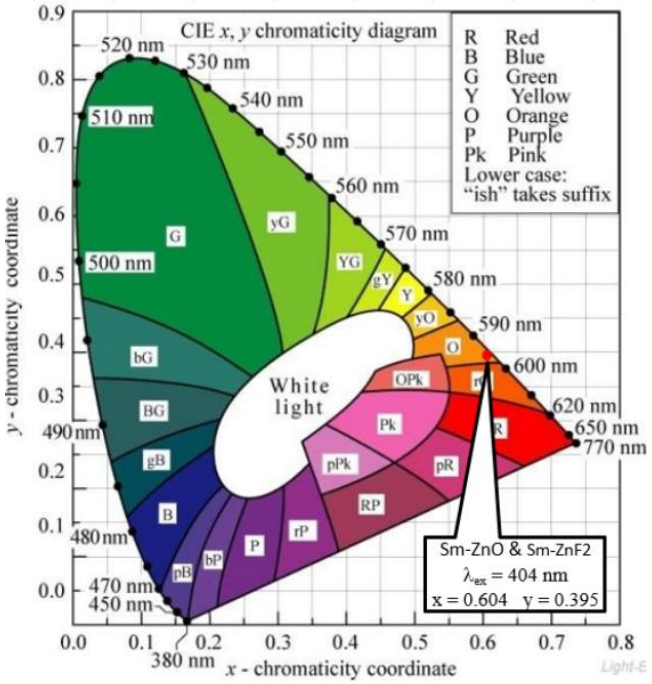


Figure 6 CIE diagram of glass comparing zinc oxide and zinc fluoride.

3.6 Lifetime

The fluorescence lifetime of the $^4G_{5/2}$ excited state of Sm^{3+} ions in TBZnO and $TBZnF_2$ glasses was measured under excitation at 404 nm, and the decay profiles are shown in Figure 7. The decay curves were analyzed using a single exponential fitting model, confirming that the radiative decay of Sm^{3+} in both glass matrices follows a mono-exponential behavior, indicative of a uniform local environment and minimal energy transfer or quenching interactions. The measured lifetimes were 0.716 ms for the TBZnO glass and 0.709 ms for the $TBZnF_2$ glass. These values are relatively close, suggesting that both host matrices provide similar relaxation dynamics for Sm^{3+} ions. The marginally longer lifetime observed in TBZnO may be due to slightly enhanced asymmetry in the oxide network, which increases the radiative transition probability and reduces non-radiative losses. The comparable lifetimes indicate low non-radiative multiphonon relaxation in both glasses, which is particularly favorable in fluoride-containing glasses due to their lower phonon energy. However, the minimal difference in lifetime between TBZnO and $TBZnF_2$ suggests that the borotellurite network dominates the phonon environment, and the influence of ZnF_2 substitution is relatively minor in this regard. These findings demonstrate that both glass systems support efficient radiative decay from the $^4G_{5/2}$ level, making them suitable candidates for use in visible-emitting photonic devices. The observed lifetimes also correlate well with the emission intensities discussed earlier, further confirming the stability and effectiveness of Sm^{3+} luminescence in these host environments.

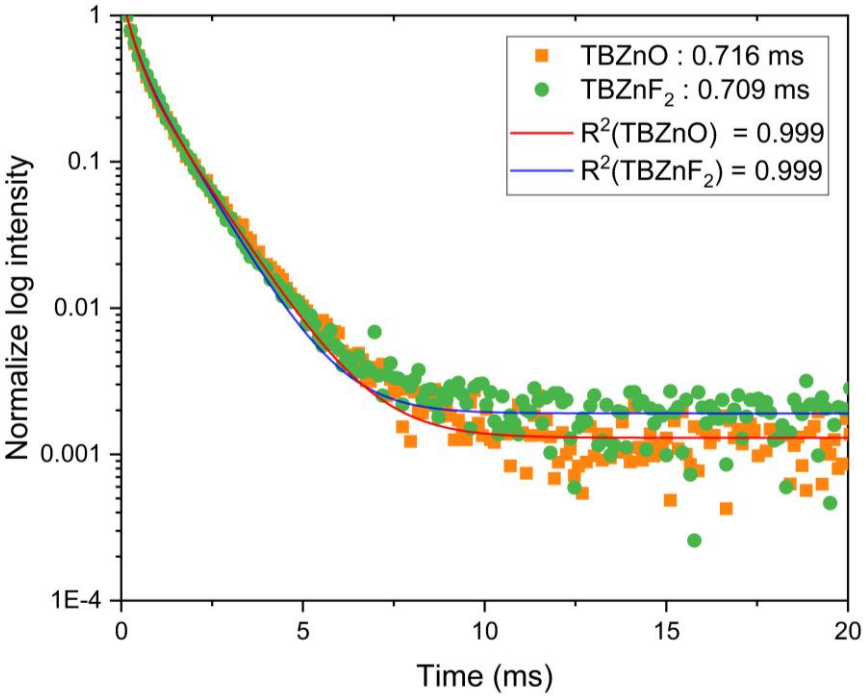


Figure 7 Lifetime of glass samples comparing zinc oxide and zinc fluoride.

3.7 Trend of result

Figure 8 presents a comparative trend between luminescence intensity, structural asymmetry, and phonon energy for Sm^{3+}-doped glasses modified with ZnO and ZnF_2 (The phonon energy values plotted are from this literature [16,17]). According to conventional understanding, the incorporation of fluoride is expected to reduce the phonon energy of the host matrix, thereby suppressing multiphonon relaxation and enhancing radiative emission. Based on this phonon-energy-driven model, the ZnF_2-containing glass should exhibit superior luminescence performance compared to the oxide-based system. However, the experimental results shown in Figure 8 clearly deviate from this expectation. Despite the lower phonon energy typically associated with fluoride-containing glasses, the ZnF_2-modified sample does not show enhanced emission intensity. Instead, the ZnO-modified glass exhibits comparable or slightly higher luminescence efficiency. This discrepancy indicates that phonon energy alone is not the dominant factor governing the luminescence behavior in the present Sm^{3+}-doped borotellurite glass system. The observed trend can be rationalized by considering the role of local structural asymmetry and bond polarizability. Experimental parameters related to disorder, such as Urbach energy, suggest that the ZnO-containing glass possesses a slightly higher degree of structural asymmetry around the Sm^{3+} ions. This asymmetry enhances the electric-dipole character of hypersensitive Sm^{3+} transitions, particularly the $^4G_{5/2} \rightarrow {}^6H_{7/2}$ emission, leading to increased radiative transition probabilities. Similar asymmetry-driven enhancement of luminescence has been reported in phospho-tellurite glasses doped with Eu^{3+}, where Judd–Ofelt parameters and EXAFS-derived disorder showed strong correlation with emission intensity [12], even in cases where phonon energy considerations alone would predict otherwise. Therefore, the trend in Figure 8 demonstrates that the luminescence efficiency of Sm^{3+}-a competition between phonon-related non-radiative relaxation and asymmetry-induced enhancement of electric-dipole transitions governs doped glasses. In this system, the latter effect dominates, resulting in a luminescence trend that contradicts the conventional phonon energy model. This finding emphasizes that, in heavy-metal oxide glass matrices, modifier-induced asymmetry and local field effects can outweigh the advantages of phonon energy reduction, providing a more comprehensive explanation for the experimental observations.

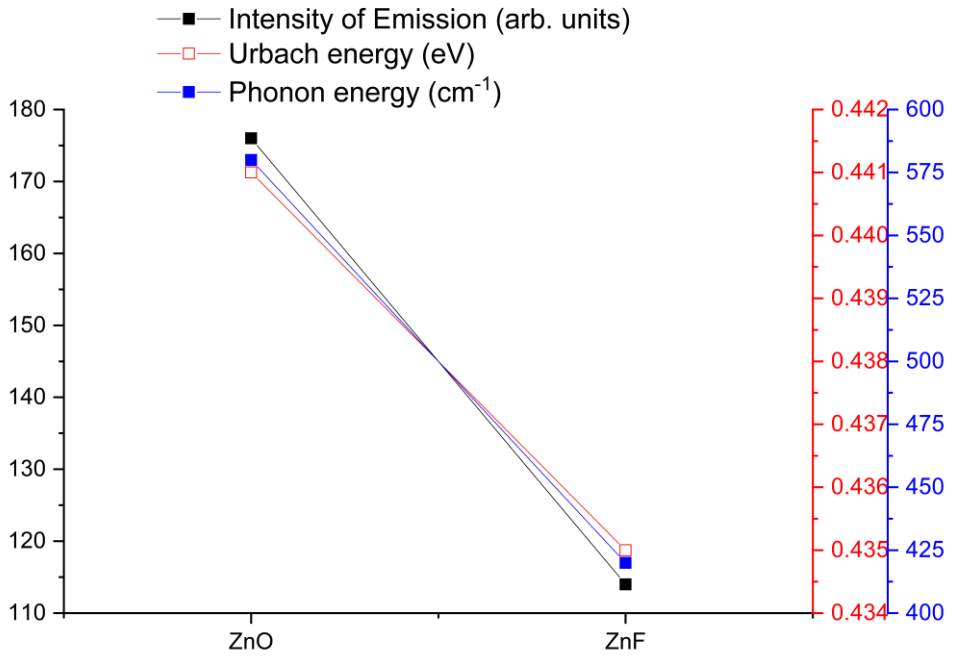


Figure 8 Trend of result between the luminescence, asymmetry and phonon energy of ZnO and ZnF_2

4. Conclusion

This study was conducted based on the common expectation that fluoride modifiers would enhance Sm^{3+} luminescence by reducing phonon energy and suppressing non-radiative relaxation. However, the experimental results show that this effect is not dominant in the present Sm^{3+}-doped borotellurite glass system. The ZnF_2-modified glass does not exhibit superior emission intensity or lifetime compared to the ZnO-modified glass. This deviation from the expected fluoride advantage can be explained by the influence of other structural factors revealed in this study. Experimental parameters related to local disorder and asymmetry, particularly the slightly higher Urbach energy observed for the ZnO-modified glass (0.441 eV) compared to the ZnF_2 glass (0.435 eV), indicate a more asymmetric and polarizable local environment around Sm^{3+} ions. Such asymmetry enhances electric dipole transition probabilities, especially for hypersensitive Sm^{3+} emissions, and compensates for the lack of phonon energy reduction. These results suggest that, in heavy metal oxide glasses, luminescence performance is governed not only by phonon energy but also by modifier-induced asymmetry and bond polarizability. Therefore, oxide modifiers such as ZnO can be more effective than fluoride modifiers for optimizing visible emission in borotellurite-based glass systems.

5. Acknowledgements

The authors express their sincere gratitude to the Center of Excellence in Glass Technology and Materials Science (CEGM) for its invaluable contribution of expertise and state-of-the-art equipment, which played a pivotal role in facilitating and advancing the research conducted in this study.

6. Author Contributions

Thanyaphirak, W.: Investigation, Data curation, Writing – original draft; Yasaka, P.: Conceptualization, Methodology, Formal analysis, Validation, Visualization, Writing – review & editing, Project administration, Supervision, Funding acquisition; Boonin, K.: Validation, Formal analysis, Writing – review & editing; Kaewkhao, J.: Conceptualization, Resources, Supervision, Project administration.

7. References

[1] Kaur A, Khanna A, Bhatt H, Gónzález-Barriuso M, González F, Chen B, et al. B O and Te O speciation in bismuth tellurite and bismuth borotellurite glasses by FTIR, 11B MAS-NMR and Raman spectroscopy. J Non Cryst Solids. 2017;470:19–26.

[2] Shaaban ER, Shapaan M, Saddeek YB. Structural and thermal stability criteria of Bi_2O_3-B_2O_3 glasses. J Phys: Condens Matter. 2008;20(15).

[3] Leśniak M, Szal R, Starzyk B, Gajek M, Kochanowicz M, Żmojda J, Miluski P, Dorosz J, Sitarz M, Dorosz D. Influence of barium oxide on glass-forming ability and glass stability of the tellurite–phosphate oxide glasses: Thermal and structural investigations. J Therm Anal Calorim. 2019;138(6):4295–4302.

[4] Iordanova R, Milanova M, Aleksandrov L, Shinozaki K, Komatsu T. Structural study of WO3-La2O3-B2O3-Nb2O5 glasses. J Non Cryst Solids. 2020;543.

[5] Anand Pandarinath M, Upender G, Narasimha Rao K, Suresh Babu D. Thermal, optical and spectroscopic studies of boro-tellurite glass system containing ZnO. J Non Cryst Solids. 2016;433:60–67.

[6] Kilic G, Issever UG, Ilik E. Synthesis, characterization and crystalline phase studies of TeO2–Ta2O5–ZnO/ZnF2 oxyfluoride semiconducting glasses. J Non Cryst Solids. 2020;527.

[7] Gunha JV, Muniz RF, Somer A, Sabino S do RF, Dias DT, El-Mallawany R, Novatski A. The effect of fluorine replacement on the physical properties of oxyfluorotellurite glasses TeO2-Li2O-ZnO-ZnF2. J Non Cryst Solids. 2023 ;603.

[8] Thanyaphirak W, Yasaka P, Sa-Ardsin W, Kaewkhao J. Concentration dependence of visible luminescence from Pr3+doped niobium zinc barium boro-tellurite glasses. In: Journal of Physics: Conference Series. Institute of Physics; 2023.

[9] Carnall WT, Fields PR, Rajnak K. Electronic Energy Levels in the Trivalent Lanthanide Aquo Ions. I. Pr3+, Nd3+, Pm3+, Sm3+, Dy3+, Ho3+, Er3+, and Tm3+. J Chem Phys. 1968;49(10):4424–42.

[10] Suaif A, Yuliantini L, Djamal M, Kaewkhao J, Yasaka P. A Comparative study of TeO2 concentration on zinc barium boro-tellurite glass doped with Sm3+. Mater Today. 2019;17:1809–1814.

[11] Ennouri M, Jlassi I, Elhouichet H, Gelloz B. Improvement of spectroscopic properties and luminescence of Er3+ions in phospho-tellurite glass ceramics by formation of ErPO4 nanocrystals. J Lumin. 2019;216.

[12] Thanyaphirak W, Yasaka P, Boonin K, Busayaporn W, Tariwong Y, Intachai N, Kothan S, Kim HJ, Kaewkhao J. Asymmetry effect on luminescence behaviors phospho-tellurite glass doped Eu3+: Judd-Ofelt analysis and EXAFS investigations. Ceram Int. 2025;51(18):25340–25350.

[13] Maheshvaran K, Linganna K, Marimuthu K. Composition dependent structural and optical properties of Sm3+ doped boro-tellurite glasses. J Lumin. 2011;131(12):2746–2753.

[14] Suaif A, Yuliantini L, Djamal M, Kaewkhao J, Yasaka P. A Comparative study of TeO2 concentration on zinc barium boro-tellurite glass doped with Sm3+. Mater Today. 2019;17:1809–1814.

[15] Krishnaiah KV, Kumar KU, Jayasankar CK. Spectroscopic properties of Dy3+-doped oxyfluoride glasses for white light emitting diodes. Materials Express. 2013;3(1):61–70.

[16] Shan W, Walukiewicz W, Ager JW, Yu KM, Yuan HB, Xin HP, Cantwell G, Song JJ. Nature of room-temperature photoluminescence in ZnO. Appl Phys Lett. 2005;86(19):1–3.

[17] Yan J, Jia Z, Wang J, Zhang C, Wang F, Mei Y, Meng F, Ohishi Y, Zhang D, Qin W, Wang F, Qin G. Efficient O-band emission from Pr3+ doped low phonon energy ZnF2-based glasses. Opt Mater (Amst). 2024;147:114764.